The 6th International Conference on Control, Instrumentation, and Automation (ICCIA2019)

ANN-Based Frequency and Tie-Line Power Control in Interconnected Microgrids

Sharara Rehimi
Rahmatollah Mirzaei
Hassan Bevrani
Smart/Micro Grids Research Center (SMGRC)
University of Kurdistan, Sanandaj, Iran

***Abstract*—Microgrids can operate in three different possible modes, including grid-connected, islanded and the interconnected operation modes. One of the big challenges in the interconnected microgrids is frequency and tie-line power control because of the nonlinearity behavior of the interconnected microgrids. Thus an adaptive controller is needed for solving this problem. In response to this challenge, in the present paper, an artificial neural network controller is presented. The control methodology is applied to two-AC interconnected microgrids considering a simplified frequency response model. The effectiveness of the proposed controller is examined by simulation. The simulation results show that in different conditions, artificial neural network controllers can operate better than the conventional proportional-integral controllers.**

***Index Terms*--Interconnected microgrids, load-frequency control, artificial neural network, simplified model, tie-line control, frequency response**

I. INTRODUCTION

Based on some drawbacks of conventional power systems and the growth of renewable energy resources (RESs) as the main components of microgrids, a number of microgrids are predicted to be used in the future [1]. Thus, the interconnected microgrids (IMGs) acquire a fundamental role in power generation and provide a better condition for power exchange [2]. The IMGs are introduced as a new structure of power grids. Although microgrids have given away to solve many problems faced by the traditional systems, they have also created some new challenges [1]. One of the main challenges in the AC microgrids is frequency deviation, especially in the interconnected operation mode. With the growth of microgrids and the creation of IMGs, the complexity of power grids increases and handling frequency and tie-line power control which is known as load-frequency control (LFC) becomes more difficult. In the IMGs, the load may vary at each microgrid as an autonomous control area. The frequency in an area is affected and then the result propagates to other connected areas through the existing tie-lines [3]. To return back to the steady-state value of the frequency after a given load variation, a control system is required to operate in each area. The LFC is an important issue in IMGs operation to obtain a reliable electric power [4]. On the other hand, up to now, there is no exact investigation on the IMGs frequency response modeling for the sake of frequency/tie-line control.

In the IMGs, frequency deviation caused by unbalancing between demand and generation that must be maintained fixed continuously and automatically [5]. In the conventional control strategy, the PI controller is used to providing zero steady-state frequency deviation [6]. But controllers which are designed based on fixed plant models, may not work when some system parameters are varying [7], and the PI controllers may provide poor dynamic performance especially for non-linearity and parameter variations. That is why these controllers are not efficient in LFC for IMGs. Furthermore, the required observer for estimating of parameters would involve an additional cost. In order to improve the system performance, adaptive control strategies have been proposed in [8, 9]. An adaptive controller is applied to make the control process sensitive to the parameters change and nonlinearities of the system [10]. The adaptive methods need the information of the system states which is not completely known due to the uncertainty of the IMGs. Thus, an artificial neural network (ANN) controller can be considered as a good solution to present an adaptive controller with improved performance.

The purpose of this paper is to present a new method of designing a decentralized LFC system for IMGs. Here, an ANN-based LFC system is designed in each microgrid. The simulation results show that the controlled IMGs using back propagation-based ANN can give desirable dynamic responses in different situations. Simulation results show that the purposed control scheme is able to provide specified objectives in the IMGs. Moreover, the response of the system employing the purposed controller seems to be insensitive to parameter changes. The proposed method is applied to two-AC IMGs.

This paper is organized as follows: the next section describes a simplified frequency response model (FRM) for IMGs. In Section III, the structure of the applied ANN controller is explained. In order to demonstrate the effectiveness of the proposed LFC system based on the simplified FRM for IMGs, some simulation results for two AC

978-1-7281-5815-0/19/$31.00©2019 IEEE

IMGs are given in Section IV. Finally, in Section V, the conclusion is presented.

II. INTERCONNECTED MICROGRIDS MODEL

The IMGs topology used in this paper is a two-area microgrids as shown in Fig. 1. Each microgrid is modeled as a DG with an equivalent inverter-based primary source and load. Here, each DG is presented by a three-phase controllable voltage source and a series RL branch, and each load is represented by a parallel RLC network [11]. The interconnected line between two microgrids is represented by a series of RL elements as shown in Fig. 2.

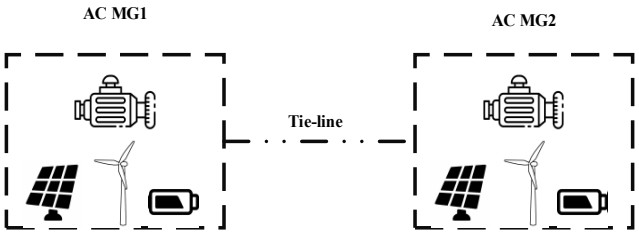

Figure 1. Two AC IMGs.

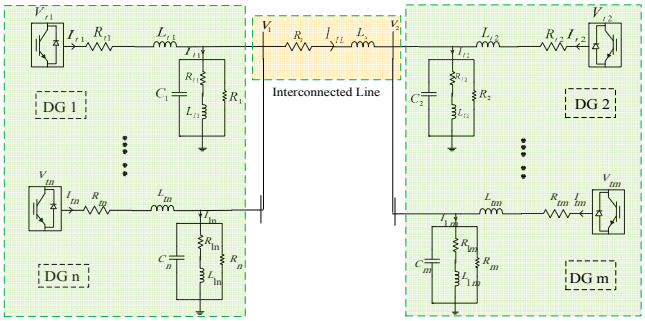

Figure 2. Circuit schematic of studied IMGs.

Based on this model, using deferential equations of this equivalent circuit in *dq0* frame, the state space of the system is obtained. For more simplification, first, each microgrid is replaced by an equivalent distributed generation as shown in Fig. 3. A, B and C matrices are presented in the appendix. Next, according to the state-space model of overall system, x, u and y are introduced as follows:

$$\begin{cases} \dot{x} = Ax + Bu \\ y = Cx \end{cases} \tag{1}$$

where

$$x^T = (I_{eqt1.d}.V_{1.d}.I_{eqt2.d}.V_{2.d}.I_{IL.d}.I_{eql1.d}.\ I_{eql2.d}.I_{eqt1.q}.V_{1.q}.\ I_{eqt2.q}.V_{2.q}.\ I_{IL.q}.I_{eql1.q}.I_{eql2.q}) \tag{2}$$

$$u^T = (V_{eqt1.d}\ .V_{eqt2.d}\ .V_{eqt1.q}.V_{eqt2.q}) \tag{3}$$

$$y^T = (V_{1.d}.V_{2.d}.V_{1.q}.V_{2.q}) \tag{4}$$

represent state-space variables, inputs and outputs vectors, respectively. To achieve a simpler FRM a sensitivity-based approach is used. A step input signal is applied and the Fast Fourier Transform (FFT) is plotted for the obtained step response. During this process, ineffective parameters on nominal frequency response are investigated. Then, these ignorable dynamics are removed and a simplified model is obtained as shown in Fig. 4.

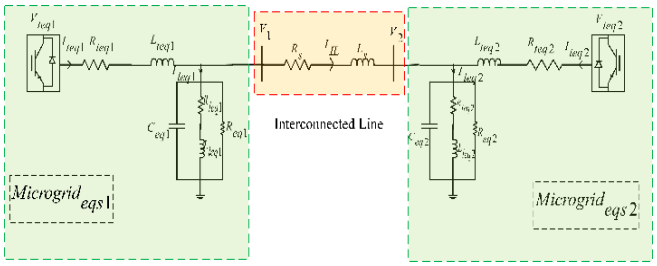

Figure 3. Equivalent circuit model for two AC IMGs.

This simplified equivalent model shows that an IMGs can be separated into three different parts as shown in Fig. 5. Based on this equivalent model, it is possible to introduce a time constant for each part as follows:

$$\begin{cases} T_{MG} = \dfrac{L_{eqt}}{R_{eqt}} \\ T_{LI} = \dfrac{L_{eql}}{R_{eql}} \\ T_{tie} = \dfrac{L_s}{R_s} \end{cases} \tag{5}$$

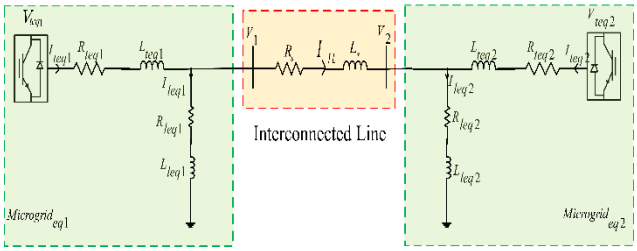

Figure 4. Simplified schematic of studied IMGs.

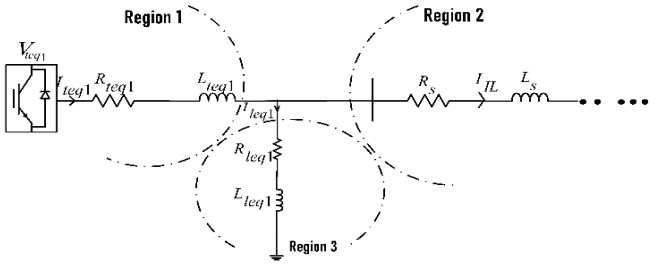

Figure 5. Three different regions of IMGs.

Here, T_{MG}, T_{IL}, and T_{tie} represent time constants of microgrid, load and inertia and interconnected line. In the simplified model, the damping factor is neglected because of its small value. Finally, IMGs can be modeled as shown in Fig. 6.

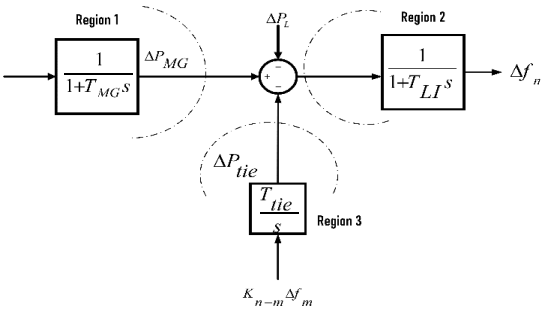

Figure 6. Block diagram of three regions of IMGs.

Finally, primary and secondary control loops are applied to the proposed model. Fig. 7. Shows the complete structure of FRM for two AC IMGs.

III. ARTIFICIAL NEURAL NETWORK CONTROLLER

In this paper, an ANN controller is used to regulate frequency on the nominal value in the secondary control level [12]. The proposed ANN controller has three layers with the backpropagation training method. ANN acts as an intelligent unit for LFC application purposes. Fig. 8 shows the basic elements of an ANN as a simple mathematical model for a neuron. Each neuron has three basic components: weights wj = [w_1 w_2 ... w_n], bias θ, and a single activation function $f_{(net)}$. Inputs x_j are multiplied by the related weight of the neuron connection. Bias θ is a magnitude offset that is applied to the activation function of the k_{th} node and output y(k) as follows [13]:

$$y_k = f\left(\sum_{j=1}^{n}\left(w_j x_j(k)\right) + \theta\right) \qquad (6)$$

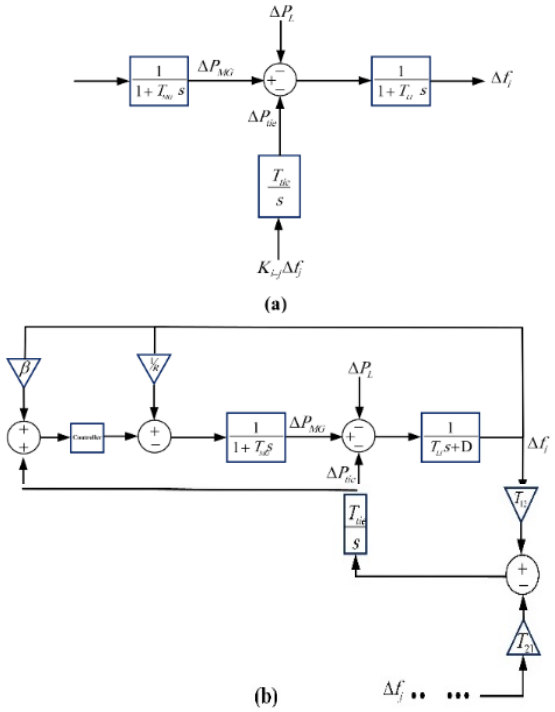

Fig. 7. Frequency response model of interconnected microgrids (a) without control layers; (b) with primary and secondary control.

The activation function can be represented as a log sigmoid, sign, tan sigmoid or other suitable functions. For some learning algorithms such as back-propagation, the derivative of the activation function $f_{0(net)}$ is necessary. Thus, differentiable activation function must be selected.

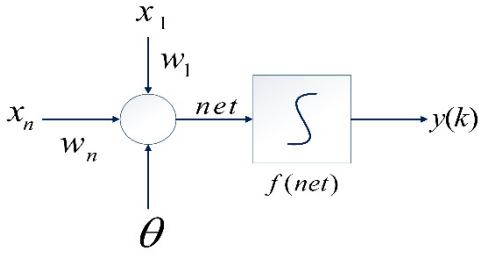

Figure 8. Simple model of a neuron.

The weights will be updated based on the following formulas:

$$\begin{cases} \Delta W_1 = -\eta \dfrac{\partial E}{\partial w_1} \\ \dfrac{\partial E}{\partial w_1} = \dfrac{\partial E}{\partial y} \cdot \dfrac{\partial y}{\partial u} \cdot \dfrac{\partial u}{\partial net_k} \cdot \dfrac{\partial net_k}{\partial H_j} \cdot \dfrac{\partial H_j}{\partial net_j} \cdot \dfrac{\partial net_j}{\partial w_1} \\ \dfrac{\partial u}{\partial net_k} = f'(net_k) \\ \dfrac{\partial net_k}{\partial H_j} = W_2 \\ \dfrac{\partial H_j}{\partial net_j} = f'(net_j) \\ \sigma_j = \delta_k \cdot W_2 \cdot f'(net_j) \\ \Delta W_1 = \eta \cdot \delta_k \cdot f'(net_k) \cdot W_2 \cdot f'(net_j) \cdot X \qquad \cdot \sigma_j \cdot X \end{cases} \tag{7}$$

$$\begin{cases} \Delta W_2 = -\eta \dfrac{\partial E}{\partial w_2} \\ \dfrac{\partial E}{\partial w_2} = \dfrac{\partial E}{\partial y} \cdot \dfrac{\partial y}{\partial u} \cdot \dfrac{\partial u}{\partial net_k} \cdot \dfrac{\partial net_k}{\partial W_2} \\ \dfrac{\partial u}{\partial net_k} = f'(net_k) \\ \dfrac{\partial net_j}{\partial w_2} = H_j \\ \dfrac{\partial E}{\partial y} \cdot \dfrac{\partial y}{\partial u} \cdot \dfrac{\partial u}{\partial net_j} = \delta_k \\ \Delta W_2 = \eta \cdot \delta_k \cdot H_j \end{cases} \tag{8}$$

The parameters which are used in the above relations are presented in Fig. 9.

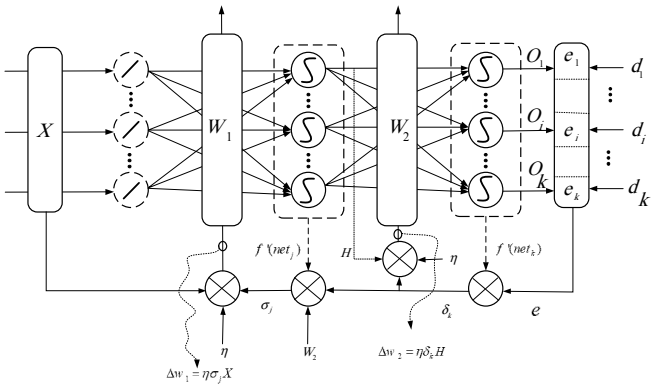

Figure 9. Process of weights updateing in back propagation method.

I. SIMULATION

In order to demonstrate the effectiveness of the proposed frequency/tie-line control scheme for IMGs, some simulations were carried out. A two IMGs have been supplemented by ANN controllers to demonstrate the performance of frequency/tie-line control system using MATLAB/Simulink environment. To illustrate the effectiveness of the proposed controller, a two-control area is considered as a test system. It is assumed that each control area is a complete microgrid. In this section, the validity of the modeling and control system is tested using two different scenarios. First, two IMGs with PI controller are simulated in MATLAB/Simulink environment, then system is tested using the proposed ANN controller.

A. Scenario I

First scenario is driven considering the same conditions for both IMGs and applying $\Delta P_L = 0 \cdot 2$ in t=2s to both microgrids. Fig. 10 shows frequency deviation and Fig. 11 shows the tie-line power deviation. It is obvious that the ANN controller provides better performance than the PI controller.

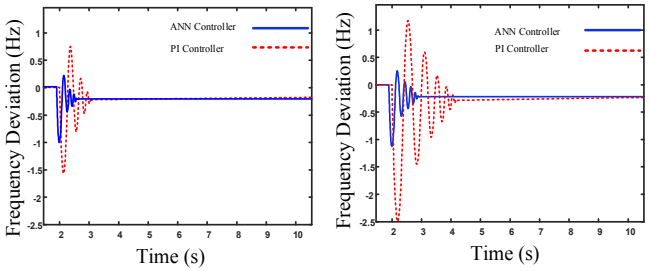

Figure 10. Performance comparison for PI and ANN controllers for frequency deviations in scenario 1, a) microgrid 1 and b) microgrid 2.

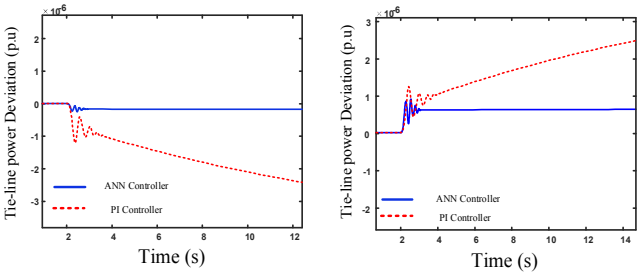

Figure 11. Performance comparison for PI and ANN controllers for tie-line power deviations in scenario 1, a) microgrid 1 and b) microgrid 2.

B. Scenario II

In this scenario, 25% increase in the value of ΔP_L in the first area and at the same time, a 30% decrease in the value of ΔP_L in the second area is accrued. As shown in Fig. 12 and Fig. 13, the PI controller is not able to maintain the system stability for frequency/tie-line power deviation.

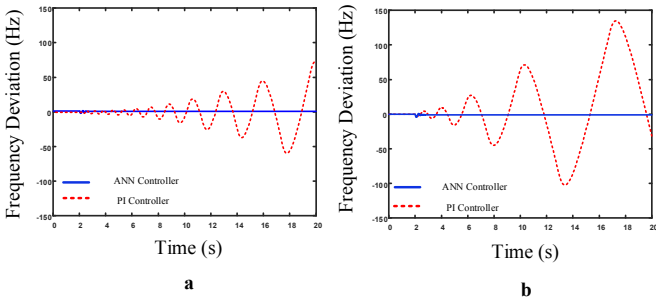

Figure 12. Performance comparison for PI and ANN controllers for frequency deviations in scenario 2, a) microgrid 1 and b) microgrid 2.

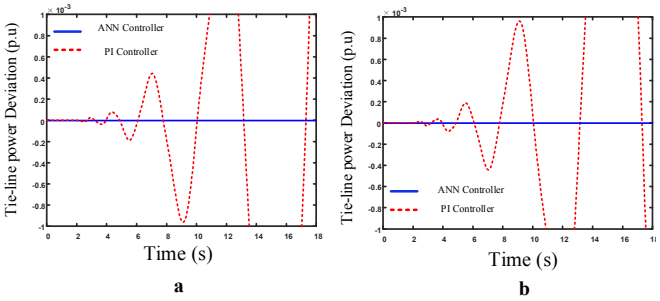

Figure 13. Performance comparison for PI and ANN controllers for tie-line power deviations in scenario 2, a) microgrid 1 and b) microgrid 2.

I. CONCLUSIONS

This study presents the application of ANN in frequency/tie-line power control of two IMGs. In practice, IMGs generally have more than two areas and each area are different from the other ones. The adaptive operation of the neural network controller is the main advantages of the proposed control strategy and the validation of the control technique is verified through extensive simulation for two IMGs. The obtained simulation results show that the performance of the ANN controller is better than conventional PI controller against to the non-linearity of the system and parameters change.

Acknowledgment

This work is supported by the Smart/Micro Grids Research Center (SMGRC), University of Kurdistan, Sanandaj, Iran.

References

[1] R. Zamora and A. K. Srivastava, "Multi-layer architecture for voltage and frequency control in networked microgrids," *IEEE Transactions on Smart Grid,* vol. 9, no. 3, pp. 2076-2085, 2016.

[2] H. Bevrani and T. Hiyama, "Bilateral-based LFC analysis using a modified conventional model," in *Proceedings 13th Iranian Conference on Electrical Engineering (ICEE)*, 2005.

[3] A. Demiroren, H. Zeynelgil, and N. Sengor, "The application of ANN technique to load-frequency control for three-area power system," in *2001 IEEE Porto Power Tech Proceedings (Cat. No. 01EX502)*, vol. 2: IEEE, p. 5 pp. vol. 2, 2001.

[4] Q. Ha and H. Trinh, "A variable structure-based controller with fuzzy tuning for load-frequency control," *International Journal of power and energy systems,* vol. 20, no. 3, pp. 146-154, 2000.

[5] X. Zhang, C. Chen, Z. Zheng, G. Strbac, and J. Kubokawa, "Allocation of frequency regulation services," in *DRPT2000. International Conference on Electric Utility Deregulation and Restructuring and Power Technologies. Proceedings (Cat. No. 00EX382)*, IEEE, pp. 349-354, 2000.

[6] T. Fernando, K. Emami, S. Yu, H. H.-C. Iu, and K. P. Wong, "A novel quasi-decentralized functional observer approach to LFC of interconnected power systems," *IEEE Transactions on Power Systems,* vol. 31, no. 4, pp. 3139-3151, 2015.

[7] K. Lim, Y. Wang, and R. Zhou, "Robust decentralised load–frequency control of multi-area power systems," *IEE Proceedings-Generation, Transmission and Distribution,* vol. 143, no. 5, pp. 377-386, 1996.

[8] I. Vajk, M. Vajta, L. Keviczky, R. Haber, J. Hetthéssy, and K. Kovacs, "Adaptive load-frequency control of the hungarian power system," *Automatica,* vol. 21, no. 2, pp. 129-137, 1985.

[9] J. Talaq and F. Al-Basri, "Adaptive fuzzy gain scheduling for load frequency control," *IEEE Transactions on power systems,* vol. 14, no. 1, pp. 145-150, 1999.

[10] H. Zeynelgil, A. Demirören, and N. Şengör, "Load frequency control for power system with reheat steam turbine and governor deadband non□linearity by using neural network controller," *European transactions on electrical power,* vol. 12, no. 3, pp. 179-184, 2002.

[11] F. Habibi, H. Bevrani, and J. MOSHTAGH, "Designing a Self-Tuning Frequency Controller Based on ANNs for an Isolated Microgrid," 2012.

[12] H. Bevrani. (2014) "Robust Power System Frequency Control-2nd Edition, Springer, (2014).

[13] S. Shokoohi, F. Sabori, and H. Bevrani, "Secondary voltage and frequency control in islanded microgrids: online ANN tuning approach," in *2014 Smart Grid Conference (SGC)*, IEEE, pp. 1-6, 2014.

Appendix

$$A=\begin{bmatrix}
\frac{-R_{eqt1}}{L_{eqt1}} & \frac{-1}{L_{eqt1}} & 0 & 0 & 0 & 0 & 0 & \omega_0 & 0 & 0 & 0 & 0 & 0 & 0\\
\frac{1}{C_{eq1}} & \frac{-1}{R_{eq1}C_{eq1}} & 0 & 0 & \frac{-1}{C_{eq1}} & \frac{-1}{C_{eq1}} & 0 & 0 & \omega_0 & 0 & 0 & 0 & 0 & 0\\
0 & 0 & \frac{-R_{eqt2}}{L_{eqt2}} & \frac{-1}{L_{eqt2}} & 0 & 0 & 0 & 0 & 0 & \omega_0 & 0 & 0 & 0 & 0\\
0 & 0 & \frac{1}{C_{eq1}} & \frac{-1}{R_{eq2}C_{eq2}} & \frac{1}{C_{eq2}} & 0 & \frac{-1}{C_{eq2}} & 0 & 0 & 0 & \omega_0 & 0 & 0 & 0\\
0 & \frac{1}{L_{eqs}} & 0 & \frac{-1}{L_{eqs}} & \frac{-R_{eqs}}{L_{eqs}} & 0 & 0 & 0 & 0 & 0 & 0 & \omega_0 & 0 & 0\\
0 & \frac{1}{L_{eql1}} & 0 & 0 & 0 & \frac{-R_{eql1}}{L_{eql1}} & 0 & 0 & 0 & 0 & 0 & 0 & \omega_0 & 0\\
0 & 0 & 0 & \frac{1}{L_{eql2}} & 0 & 0 & \frac{-R_{eql2}}{L_{eql2}} & 0 & 0 & 0 & 0 & 0 & 0 & \omega_0\\
-\omega_0 & 0 & 0 & 0 & 0 & 0 & 0 & \frac{-R_{eqt1}}{L_{eqt1}} & \frac{-1}{L_{eqt1}} & 0 & 0 & 0 & 0 & 0\\
0 & -\omega_0 & 0 & 0 & 0 & 0 & 0 & \frac{1}{C_{eq1}} & \frac{-1}{R_{eq1}C_{eq1}} & 0 & 0 & \frac{-1}{C_{eq1}} & \frac{-1}{C_{eq1}} & 0\\
0 & 0 & -\omega_0 & 0 & 0 & 0 & 0 & 0 & 0 & \frac{-R_{eql2}}{L_{eql2}} & \frac{-1}{L_{eqt2}} & 0 & 0 & 0\\
0 & 0 & 0 & -\omega_0 & 0 & 0 & 0 & 0 & 0 & \frac{1}{C_{eq2}} & \frac{-1}{R_{eq2}C_{eq2}} & \frac{1}{C_{eq2}} & 0 & \frac{-1}{C_{eq2}}\\
0 & 0 & 0 & 0 & -\omega_0 & 0 & 0 & 0 & \frac{1}{L_{eqs}} & 0 & \frac{-1}{L_{eqs}} & \frac{-R_{eqs}}{L_{eqs}} & 0 & 0\\
0 & 0 & 0 & 0 & 0 & -\omega_0 & 0 & 0 & \frac{1}{L_{eql1}} & 0 & 0 & 0 & \frac{-R_{eql1}}{L_{eql1}} & 0\\
0 & 0 & 0 & 0 & 0 & 0 & -\omega_0 & 0 & 0 & 0 & \frac{1}{L_{eql2}} & 0 & 0 & \frac{-R_{eql2}}{L_{eql2}}
\end{bmatrix}$$

$$B=\begin{bmatrix}
\frac{1}{L_{eqt1}} & 0 & 0 & 0\\
0 & 0 & 0 & 0\\
0 & \frac{1}{L_{eqt2}} & 0 & 0\\
0 & 0 & 0 & 0\\
0 & 0 & 0 & 0\\
0 & 0 & 0 & 0\\
0 & 0 & 0 & 0\\
0 & 0 & \frac{1}{L_{eqt1}} & 0\\
0 & 0 & 0 & \frac{1}{L_{eqt2}}\\
0 & 0 & 0 & 0\\
0 & 0 & 0 & 0\\
0 & 0 & 0 & 0\\
0 & 0 & 0 & 0
\end{bmatrix}$$

$$C=[0\,1\,0\,0\,0\,0\,0\,0\,0\,0\,0\,0\,0\,0]$$